An Accurate Model for EESM and its Application to Analysis of CQI Feedback Schemes and Scheduling in LTE

Sushruth N. Donthi and Neelesh B. Mehta, *Senior Member, IEEE*

***Abstract*—The Effective Exponential SNR Mapping (EESM) is an indispensable tool for analyzing and simulating next generation orthogonal frequency division multiplexing (OFDM) based wireless systems. It converts the different gains of multiple subchannels, over which a codeword is transmitted, into a single effective flat-fading gain with the same codeword error rate. It facilitates link adaptation by helping each user to compute an accurate channel quality indicator (CQI), which is fed back to the base station to enable downlink rate adaptation and scheduling. However, the highly non-linear nature of EESM makes a performance analysis of adaptation and scheduling difficult; even the probability distribution of EESM is not known in closed-form. This paper shows that EESM can be accurately modeled as a lognormal random variable when the subchannel gains are Rayleigh distributed. The model is also valid when the subchannel gains are correlated in frequency or space. With some simplifying assumptions, the paper then develops a novel analysis of the performance of LTE's two CQI feedback schemes that use EESM to generate CQI. The comprehensive model and analysis quantify the joint effect of several critical components such as scheduler, multiple antenna mode, CQI feedback scheme, and EESM-based feedback averaging on the overall system throughput.**

***Index Terms*—Effective exponential SNR mapping (EESM), long term evolution (LTE), orthogonal frequency division multiplexing (OFDM), channel quality feedback, multiple antenna diversity, frequency-domain scheduling, adaptive modulation and coding, lognormal random variable.**

I. Introduction

ORTHOGONAL frequency division multiplexing (OFDM) is the downlink access technique of choice in wideband wireless cellular standards such as Long Term Evolution (LTE) [1] and IEEE 802.16e WiMAX. In an OFDM downlink, the base station (BS) simultaneously serves multiple users on orthogonal subcarriers. The scheduler at the BS exploits the frequency-selective nature of the wideband channel and multi-user diversity. By adapting the data rate, it also takes advantage of the time-varying nature of the channel.

A key step in rate adaptation involves determining the modulation and coding scheme (MCS). It is chosen in order to maximize the data rate to the scheduled user subject to a constraint on the probability of codeword error [2]. Since a codeword is encoded across multiple, say N, subcarriers, this determination would first require a characterization of the codeword error rate as a function of the N different subcarrier gains. Thus, rate adaptation requires an N-dimensional look up table, which is cumbersome to generate, store, and use.

This difficulty has motivated the widespread use of the Effective Exponential Signal-to-noise-ratio (SNR) Mapping (EESM). EESM maps the SNRs of the N subcarriers, $X_1, X_2, \ldots, X_N$, to a single *effective SNR* X_{eff} as follows [3], [4]:[1]

$$X_{\text{eff}} = -\lambda \ln\left(\frac{1}{N}\sum_{l=1}^{N} e^{-\frac{X_l}{\lambda}}\right), \tag{1}$$

where λ is a parameter that is empirically calibrated as a function of the MCS and packet length. The effective SNR is interpreted as the SNR seen by the codeword as if it were transmitted over a flat-fading channel. While the reduction of N variables to a single variable is empirical and not information lossless, several studies have shown that EESM is an accurate indicator of the codeword error rate [4]. Thus, only a single variable, X_{eff}, needs to be dealt with for rate adaptation and scheduling. EESM is also a critical component in OFDM system-level simulators, which simulate the performance of a cellular system that consists of multiple cells and BSs that serve multiple users, and makes large system-level simulations computationally feasible. Consequently, it was extensively used during the LTE standardization deliberations [6].

Another important and different use of EESM, which motivates this paper, arises in the generation of channel quality information by the user equipments (UEs). It is fed back by the UEs via the uplink and is then used by the BS for frequency-domain scheduling and for rate adaptation on the downlink. Such feedback is needed because the uplink and downlink channels are not reciprocal.[2] As a result, the BS does not

Manuscript received December 19, 2010; revised May 8, 2011 and July 1, 2011; accepted July 1, 2011. The associate editor coordinating the review of this paper and approving it for publication was I.-M. Kim.

S. N. Donthi is with Broadcom Corp., Bangalore, India. He was with the Dept. of Electrical Communication Eng., Indian Institute of Science (IISc), Bangalore, India during the course of this work (e-mail: dnsushruth@gmail.com).

N. B. Mehta is with the Dept. of Electrical Communication Eng., IISc, Bangalore, India (e-mail: nbmehta@ece.iisc.ernet.in).

This work was partially supported by a project funded by the Ministry of Information Technology, India.

Digital Object Identifier 10.1109/TWC.2011.081011.102247

[1]Note that other functional forms for EESM have also been proposed, e.g., [5]. We use (1) given its widespread use.

[2]The uplink and downlink channels are clearly not reciprocal in the frequency division duplex (FDD) mode. Even in the time division duplex (TDD) mode, they are not reciprocal due to asymmetry in interference and transmit and receive radio circuitries.

know a priori the channel gains of the subcarriers for any UE.

Since subcarrier-level feedback consumes considerable uplink bandwidth, several feedback reduction techniques are used in practice [7]–[9]. For example, in the subband-level channel quality indicator (CQI) feedback scheme specified in LTE, each UE feeds back only one 4-bit CQI for every subband. A subband is defined to be a collection of $q \geq 2$ physical resource blocks (PRBs), and each PRB consists of 12 contiguous subcarriers. While the frequency response of the channel is typically flat across a 180 kHz wide PRB, it is not flat across a subband, which can have a bandwidth as large as 1 MHz. Therefore, the UE uses EESM to compute the effective SNR for each subband and then determines the appropriate MCS. When the channel is frequency-flat across a PRB, the effective subband SNR is a function of q SNR values. The computed MCS is fed back to the frequency-domain scheduler at the BS, which then assigns appropriate UEs to different PRBs. In the UE selected subband feedback scheme of LTE, which is described in detail below, the EESM gets computed over an even larger number of PRB SNRs.

The performance of the CQI feedback schemes, therefore, depends on the statistics of the effective SNR generated by EESM. However, the non-linear nature of (1) makes an exact analysis intractable. In fact, even the probability distribution function (PDF) of EESM is not known in closed-form. While expressions for its moment generating function (MGF) and moments are available [10], they are quite involved. The EESM was approximated by a Gaussian or a logarithm of a Gaussian (log-Gaussian) random variable (RV) in [11]; however, its accuracy, as we shall see, is poor.[3]

One can, therefore, see that it is quite a challenge to analyze the performance of next generation OFDM systems, such as LTE, that use a spectrally efficient combination of rate adaptation, multiple antenna techniques, and frequency-domain scheduling, and employ EESM to generate CQI feedback. Consequently, most papers that deal with scheduling, adaptation, or CQI feedback for the LTE downlink resort to simulations [9], [12]–[14]. For example, in [13], contiguous and distributed subcarrier allocations are compared by simulations, and their effects on the throughput of greedy and proportional fair (PF) schedulers is evaluated. In [9], the performance of a PF scheduler was studied assuming that it has access to PRB-level CQI feedback.

In [15], a scheme in which each user feeds back the indices of a pre-specified number of subcarriers with the highest gains and the BS uses BPSK modulation and a round-robin scheduler to transmit, was analyzed. However, rate adaptation, multiple antenna diversity, and channel-aware scheduling were not modeled. The analysis in [16] quantified the performance gains from MIMO and rate adaptation in a cellular system, but did not consider OFDM. For a MIMO-OFDM system that uses orthogonal space-frequency block codes, [17] analyzed the performance of a greedy scheduler and used simulations to study a PF scheduler. However, one-bit feedback without rate adaptation was assumed. Neither the coarse frequency granularity of feedback nor EESM-based CQI feedback generation are considered by the above analysis papers.

A modified PF scheduler was proposed for a scheme similar to the UE selected feedback scheme in [18]. However, EESM was not considered and the analysis was limited to determining the fading-averaged probability that channel information about a given number of clusters of subcarriers is fed back. While [19]–[21] did model the coarseness, the arithmetic mean (AM) of the subcarrier SNRs was used. The AM is less accurate than the EESM [3], but entails a simpler and easier analysis. While [11] did consider EESM, aspects such as dynamic rate adaptation, scheduling, feedback, and multiple antenna diversity were not analyzed. Altogether, the simple cell planning model of [11] is quite different from ours.

A. Contributions of the Paper

Motivated by the goal of analyzing the CQI feedback techniques of LTE, we propose the use of an analytically tractable lognormal distribution to characterize the PDF of the effective SNR. This is shown to be accurate when the frequency-flat channel response across a PRB is a Rayleigh RV and the channel responses of different PRBs are mutually independent [8], [15], [22], [23]. It is also accurate when multiple antenna diversity techniques, which affect the statistics of the SNR of each PRB, are employed. Furthermore, the model is valid even in the presence of frequency-domain correlation or spatial correlation. Note that the lognormal model has been used earlier in the literature, for example, to approximate the distribution of sums of lognormal or Suzuki RVs [24], [25]. However, to the best of our knowledge, this is the first time that it has been successfully applied to model EESM.

The second major contribution of the paper is a novel and comprehensive analysis of the throughput of LTE feedback schemes that use EESM to generate CQI to enable scheduling and rate adaptation at the BS. While we focus on the PF scheduler due to space constraints, the analysis can be generalized to handle the greedy and round-robin schedulers, which trade-off fairness and throughput differently. The paper analyzes both the subband-level and the UE selected CQI feedback schemes of LTE and accounts for its different multi-antenna diversity modes. Another important aspect of this analysis is its handling of the coarse frequency granularity of the EESM-based CQI feedback, which can occasionally lead to an incorrect choice of the MCS. This aspect is novel compared to conventional rate adaptation and scheduling problems [2], [17].

Altogether, the analysis quantifies, for the first time, the joint effect of several critical components such as scheduler, multiple antenna mode, CQI feedback scheme, and EESM-based feedback averaging on the throughput of an OFDM system that is as technologically rich and as practically relevant as LTE. These components have hitherto been analyzed in isolation in the literature. The analysis also enables an optimization of the parameters associated with the CQI feedback scheme. The proposed lognormal model for EESM plays a crucial role in this analysis. Therefore, the lognormal model is accurate, analytically tractable, and useful.

The paper is organized as follows. We first discuss the CQI model of LTE in Sec. II. In Sec. III, the lognormal model

[3]In [11], the sum $\frac{1}{N}\sum_{l=1}^{N} e^{-\frac{X_l}{\lambda}}$ was approximated by lognormal and Gaussian RVs. Since the effective SNR is the logarithm of this sum, we shall instead refer to these as Gaussian and log-Gaussian approximations, respectively.

for EESM is proposed and used to analyze the LTE CQI feedback schemes. Numerical results and our conclusions follow in Sec. IV and Sec. V, respectively. Several mathematical derivations are relegated to the Appendix.

II. Model for EESM-Based CQI Feedback in LTE

We now briefly describe relevant details of the LTE downlink, such as its frame structure and its CQI feedback mechanisms, and set up the system model and notation. We use the following notation henceforth. The probability of an event A is denoted by $\Pr(A)$. For an RV X, $f_X(.)$ denotes its PDF and $\mathbb{E}[X]$ its mean. The conditional expectation of X given event A is denoted by $\mathbb{E}[X|A]$, and $\Pr(B|A)$ denotes the conditional probability of event B given A. For a set $\mathcal{I}$, $|\mathcal{I}|$ shall denote its cardinality. The set $\{x_1, x_2, \ldots, x_i\}$ is denoted by $\{x_l\}_{l=1}^{i}$.

In LTE, each downlink frame is 10 ms long and consists of ten subframes. Each subframe has a duration of 1 ms, and consists of two 0.5 ms slots. Each slot contains seven OFDM symbols. In the frequency domain, the system bandwidth, B, is divided into several orthogonal subcarriers. Each subcarrier has a bandwidth of 15 kHz. A set of twelve consecutive subcarriers over the duration of one slot is called a *Physical Resource Block (PRB)*. Let N_{PRB} denote the total number of PRBs available over the system bandwidth. Let K denote the number of UEs in a cell.

The BS is equipped with N_{t} transmit antennas and each UE has N_{r} receive antennas. In LTE, both single-stream and multiple-stream transmissions are possible. In a single-stream transmission, diversity based multiple antenna techniques are used to transmit one codeword of data. Multiple-stream transmission refers to the use of spatial multiplexing techniques to transmit two codewords of data simultaneously. In this paper, we focus on single-stream transmission in order to avoid digressing into design issues related to codebook-based transmit precoding of LTE. We cover the following modes of operation: single input single output (SISO) ($N_{\text{t}} = N_{\text{r}} = 1$), single input multiple output (SIMO) ($N_{\text{t}} = 1$ and $N_{\text{r}} \geq 2$), closed-loop and open-loop multiple input single output (MISO) ($N_{\text{t}} \geq 2$ and $N_{\text{r}} = 1$), and single-stream multiple input multiple output (MIMO) ($N_{\text{t}} \geq 2$ and $N_{\text{r}} \geq 2$).

Since the PRB bandwidth is only 180 kHz, it is justifiable to assume that the channel response is frequency-flat across all the 12 subcarriers of the PRB.[4] Let $h_{n,k}(l, j)$ denote the channel gain from the j^{th} transmit antenna of the BS to the l^{th} receive antenna of the k^{th} UE for the n^{th} PRB. It is modeled as a zero-mean circular symmetric complex Gaussian RV with variance σ_k^2, which implies that its amplitude is Rayleigh distributed. The variance depends upon shadowing and the distance between the k^{th} UE and the BS. The SNR of the n^{th} PRB of the k^{th} UE is denoted by $\gamma_{n,k}$, and depends on $h_{n,k}(l, j)$, $1 \leq l \leq N_r$, $1 \leq j \leq N_t$, and the multiple antenna mode used.

A. Channel Quality Indicator (CQI) Feedback

The CQI is a 4-bit value that indicates an estimate of the MCS that the UE can receive reliably from the BS. It is typically based on the measured received signal quality, which can be estimated, for example, using the reference signals transmitted by the BS. The number of MCSs is denoted by L and equals $2^4 = 16$. These are tabulated in [26, Tbl. 7.2.3-1]. The BS controls how often and when the UE feeds back CQI. The finest possible frequency resolution for CQI reporting is a subband, which consists of q contiguous PRBs, where $2 \leq q \leq 8$. The total number of subbands is $S = \lceil N_{\text{PRB}}/q \rceil$, where $\lceil . \rceil$ denotes the ceil function.

Let r_i denote the rate in bits/symbol achieved by the MCS corresponding to the i^{th} CQI value. To simplify notation, the subband that contains the n^{th} PRB is denoted by $s(n)$. PRBs $1, \ldots, q$ shall belong to subband 1, PRBs $q+1, \ldots, 2q$ shall belong to subband 2, and so on.

B. CQI Feedback Generation

LTE specifies two different feedback schemes to facilitate frequency-domain scheduling:[5]

- *UE selected subband CQI feedback*, in which the UE reports the positions of $M < S$ subbands that have the highest CQIs and only a single CQI value that indicates the channel quality that is averaged over all these M subbands.
- *Subband-level CQI feedback*, in which the UE reports the CQI for each of the S subbands.

Thus, the subband-level feedback scheme generates more feedback. *Both the schemes use EESM to generate the CQI value(s) from the SNRs of the PRBs that constitute the subbands.* They are illustrated in Figure 1, and are described mathematically below.

1) UE Selected Subband Feedback: The subband SNR, $\gamma_{s,k}^{\text{sub}}$, of the k^{th} UE for subband s is the effective SNR over its constituent PRBs. It is computed using EESM as

$$\gamma_{s,k}^{\text{sub}} = -\lambda \ln \left(\frac{1}{q} \sum_{n \in \mathcal{PRB}(s)} e^{-\frac{\gamma_{n,k}}{\lambda}} \right), \tag{2}$$

where $\mathcal{PRB}(s)$ denotes the set of PRBs in subband s.

Remark 1: The parameter λ needs to be empirically fine-tuned as a function of MCS and packet length [4]. However, in order to ensure analytical tractability, the parameter λ is taken to be the same for all rates. This has also been assumed in [11] to handle different codeword sizes for QPSK for which λ is different.

The k^{th} UE then orders the subband SNRs of its S subbands as $\gamma_{(1),k}^{\text{sub}} \geq \cdots \geq \gamma_{(M),k}^{\text{sub}} \geq \cdots \geq \gamma_{(S),k}^{\text{sub}}$, where (l), following standard order statistics notation, is the index of the subband with the l^{th} largest SNR. It reports the set $\mathcal{I}_k = \{(1), \ldots, (M)\}$, which consists of the M subbands with the highest CQIs. It also reports a *single* CQI, C_k^{bestM}, which can take one of 16 possible values. It is a function of the

[4]This assumption will not hold for highly dispersive channels with a delay spread greater than 5 μs, which is close to the normal cyclic prefix duration of an OFDM symbol in the LTE downlink.

[5]The standard also defines a third wideband feedback scheme, in which just one CQI value is sent for the entire system bandwidth. We do not discuss it as it not meant for frequency-domain scheduling. For both UE selected feedback and subband-level feedback, LTE reduces the CQI overhead further, while incurring a negligible performance loss, by using a 2-bit differential CQI value for each subband. It also communicates one wideband CQI value that is averaged over the whole system bandwidth.

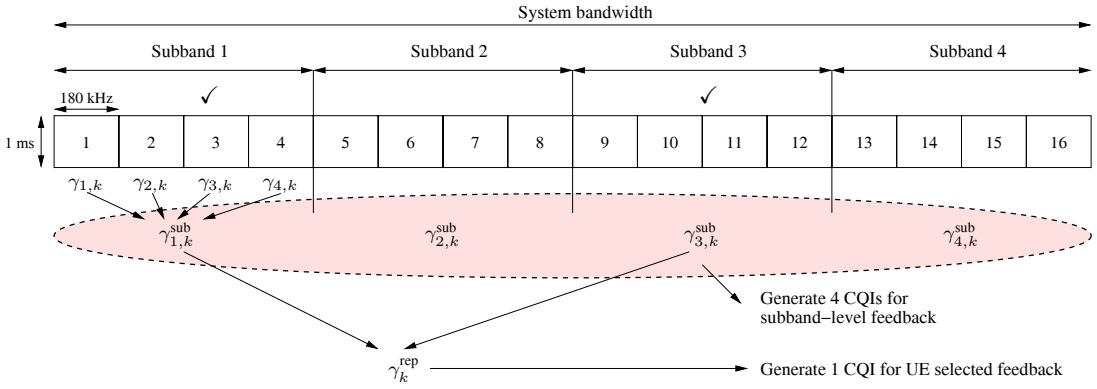

Fig. 1. An illustration of the UE selected subband feedback and subband-level CQI feedback schemes of LTE for the k^{th} UE ($S = 4$, $M = 2$, and $q = 4$). The checkmarks (✓) illustrate subbands with the M highest effective SNRs whose CQI is reported in the UE selected subband feedback scheme. The subband-level feedback scheme generates CQI for all the four subband SNRs. Each subband SNR itself is computed using EESM from the SNRs of the $q = 4$ PRBs that constitute the subband. Also shown is γ_k^{rep}, which is computed from $\gamma_{1,k}^{\text{sub}}$ and $\gamma_{3,k}^{\text{sub}}$ using EESM and is used by the UE selected subband scheme to generate one CQI.

effective SNR γ_k^{rep} that is calculated using EESM over its M selected subbands as follows:

$$\gamma_k^{\text{rep}} = -\lambda \ln \left(\frac{1}{M} \sum_{v \in \mathcal{I}_k} e^{-\frac{\gamma_{v,k}^{\text{sub}}}{\lambda}} \right). \tag{3}$$

For example, in Figure 1, $q = 4$, $M = 2$, and $\mathcal{I}_k = \{1, 3\}$.

The CQI fed back is $C_k^{\text{bestM}} = r_i$, if $\gamma_k^{\text{rep}} \in [T_{i-1}, T_i)$. Here, $T_0, T_1, \ldots, T_{L-1}, T_L$ (where $T_L = \infty$) are the link adaptation thresholds that ensure that a target block error rate is met should the BS transmit over all its M best subbands [1], [26]. For ease of explanation, we henceforth do not distinguish between r_i and its 4-bit CQI index i.

2) Subband-Level Feedback: Unlike the UE selected subband scheme, here the k^{th} UE reports a separate CQI, $C_{s,k}^{\text{sub}}$, for every subband s. It is based on $\gamma_{s,k}^{\text{sub}}$ (which is given in (2)). The CQI fed back is $C_{s,k}^{\text{sub}} = r_i$, if $\gamma_{s,k}^{\text{sub}} \in [T_{i-1}, T_i)$. As before, $C_{s,k}^{\text{sub}}$ also takes one of 16 possible values. It can be different for different subbands.

C. Frequency-Domain Scheduling

Based on the CQI reports from all the UEs, the scheduler in the BS decides which PRB to allocate to which UE.[6] The BS then signals on the downlink control channel the specific PRBs that are allocated to different UEs [1, Sec. 9.3.3]. The scheduler is not specified in the standard and is implementation-dependent. Due to space constraints, we focus on the PF scheduler as it exploits multi-user diversity while also ensuring fairness [27]–[29].

1) Using UE Selected Subband CQI Feedback: The BS uses $\mathcal{I}_k$ and C_k^{bestM} reported by all the K UEs to determine which UE to assign to each PRB. Recall that $s(n)$ denotes the subband that contains PRB n. Let $\mathcal{Z}_{s(n)}$ denote the subset of UEs that have reported the subband $s(n)$ as one of their best M subbands. The PF scheduler [28] assigns the n^{th} PRB to UE $k^*(n)$, where

$$k^*(n) = \arg \max_{k \in \mathcal{Z}_{s(n)}} \frac{C_k^{\text{bestM}}}{\mathbb{E}\left[C_k^{\text{bestM}}\right]}, \tag{4}$$

[6]In LTE, a pair of PRBs that span a duration of 1 ms are assigned together. For brevity, we refer to the pair as a PRB.

and $\mathbb{E}\left[C_k^{\text{bestM}}\right]$ is the average rate reported by the k^{th} UE. Thus, a PRB gets assigned to the UE whose CQI exceeds its mean rate the most. This ensures fairness across UEs with different mean rates.

Different versions of PF schedulers have been considered in the literature. In practice, the moving window average is used instead of $\mathbb{E}\left[C_k^{\text{bestM}}\right]$ in the denominator of (4) [22], [29]. Our model accurately models window averaging for window sizes as small as 50 [30]. In [31], the ratio of instantaneous SNR to its time-averaged value is used instead. However, these versions share similar characteristics such as allotting almost the same amount of time to each user.

Outage: Since the CQI value corresponds to the effective SNR for the best M subbands, the SNR of the n^{th} PRB may be less than the lower threshold of the MCS being used for the PRB. This causes an outage, and the throughput is 0 in that subframe. Outage for the n^{th} PRB also occurs if $\mathcal{Z}_{s(n)}$ is a null set since the PRB is then not allocated to any UE.[7]

2) Using Subband-Level CQI Feedback: The PF scheduler uses $C_{s,k}^{\text{sub}}$ reported by all the UEs to allocate the PRBs in a subband. PRB n, which lies in subband $s(n)$, is assigned to UE $k^*(n)$, where

$$k^*(n) = \arg \max_{1 \le k \le K} \frac{C_{s(n),k}^{\text{sub}}}{\mathbb{E}\left[C_{s(n),k}^{\text{sub}}\right]}. \tag{5}$$

The BS then transmits data on PRB n to UE $k^*(n)$ at a rate $C_{s(n),k^*(n)}^{\text{sub}}$. As before, if the SNR for a PRB is less than the lower threshold of the MCS used for it, then the PRB is in outage.

III. Statistical Model for EESM and its Role in LTE Throughput Analysis

For both the CQI feedback schemes, we saw that EESM plays a crucial role in the generation of CQI of a subband from the SNRs of its constituent PRBs. An analytically tractable statistical characterization of EESM is, therefore, essential in

[7]Making a UE feed back, in addition, the CQI averaged over the entire system bandwidth can mitigate this outage further since it gives the BS partial knowledge about the CSI of the PRBs.

order to analyze the performance of the feedback schemes. To this end, we first propose a new tractable statistical model for EESM and verify its accuracy. We then apply it to analyze the system throughput in Sec. III-C.

A. Statistical Model for EESM

As stated earlier, a closed-form expression for the PDF of X_{eff}, which is computed from the PRB SNRs $X_1, \ldots, X_N$ using (1), is not known because of the highly non-linear nature of the EESM mapping. We propose modeling X_{eff} as a lognormal RV, which can be written as e^G, where G is a Gaussian RV with mean μ and standard deviation Ω. Therefore, the PDF, $f_{X_{\text{eff}}}(x)$, of X_{eff} is approximated as

$$f_{X_{\text{eff}}}(x) \approx \frac{1}{x\Omega\sqrt{2\pi}} e^{-\frac{(\ln x-\mu)^2}{2\Omega^2}}, \quad x \geq 0. \tag{6}$$

By matching the first two moments of X_{eff} and e^G, it can be shown that

$$\mu = \ln\left(\mathbb{E}\left[X_{\text{eff}}\right]\right) - \frac{\Omega^2}{2}, \quad \text{and} \tag{7}$$

$$\Omega = \sqrt{\ln\left(\frac{\mathbb{E}\left[X_{\text{eff}}^2\right] - \left(\mathbb{E}\left[X_{\text{eff}}\right]\right)^2}{\left(\mathbb{E}\left[X_{\text{eff}}\right]\right)^2} + 1\right)}. \tag{8}$$

The two parameters μ and Ω shall henceforth be referred to as the *lognormal parameters of X_{eff} over its constituents* $X_1, \ldots, X_N$. The two moments $\mathbb{E}\left[X_{\text{eff}}\right]$ and $\mathbb{E}\left[X_{\text{eff}}^2\right]$, which are required in (8), are computed using one of the following two different methods.

1) Using Analytical Formulae: Expressions for the moment generating function (MGF) and the moments of X_{eff} for correlated Nakagami-m fading are derived in [10]. However, these expressions are quite involved. For example, an N-fold summation, in which each summation is over a variable set of limits, and a summation over $N!$ permutation terms are required in [10, (47), (48), (50), and (52)] to compute the first two moments.

2) Using Monte Carlo Integration Methods: An attractive alternative is the use of efficient Monte Carlo methods [32] to compute the moments of X_{eff}. In it, several samples of the subcarrier SNRs are generated and empirical moments of X_{eff} are computed to approximate the actual moments. The accuracy of this method depends on the sample size, W. Notably, the approximation error decreases as $O(W^{-\frac{1}{2}})$, and does not depend on N [32]. Such methods have been put to good use in communication-theoretic literature, see, for example, [33], [34]. We have found that a sample size of $W = 5000$ is sufficient to compute the moments accurately enough for our analysis. Note that these computations need to be carried out only once in our analysis. Further, this approach can be easily applied for any joint probability distribution of the PRB SNRs.

B. Empirical Verification of Lognormal Model for EESM

We verify the model using two different methods. The first method follows the convention used in lognormal approximation literature [24], [25]. It compares the cumulative distribution function (CDF) and the complementary CDF (CCDF) of the lognormal model for X_{eff} with its empirical CDF and CCDF, which are generated from 10^6 samples. Small values of the CDF reveal the accuracy in tracking the probability of smaller X_{eff} values. Since all CDFs saturate to 1 for large X_{eff} values, the accuracy in tracking the probability distribution of larger X_{eff} values is revealed by studying the CCDF instead. The comparison is done in Figures 2 and 3 when the PRB SNRs are exponential RVs, *i.e.*, squares of Rayleigh RVs (which also are Chi-square RVs with $\tau = 2$). The constituent SNRs are independent and identically distributed (i.i.d.) exponential RVs with mean 10 dB. Also plotted are the CDF and CCDF of the Gaussian and log-Gaussian models of [11]. We notice that the lognormal approximation, while not perfect, tracks both the CDF and CCDF of EESM well and is significantly better than the Gaussian and log-Gaussian approximations for both the CDF and the CCDF.

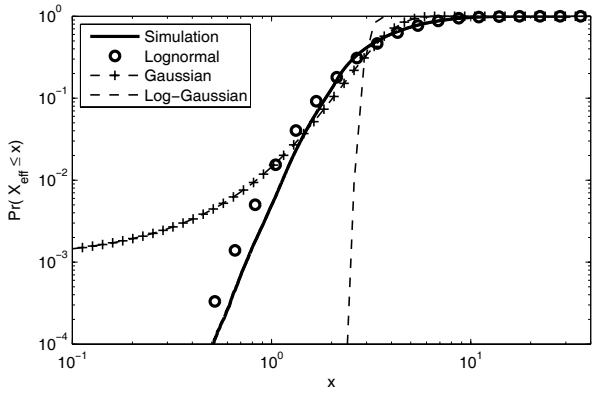

Fig. 2. Verification of the accuracy of the CDF generated by the proposed lognormal model for EESM and comparison with other proposed distributions ($\sigma^2 = 10$ dB, $\tau = 2$, $\lambda = 1.5$, and $N = 4$).

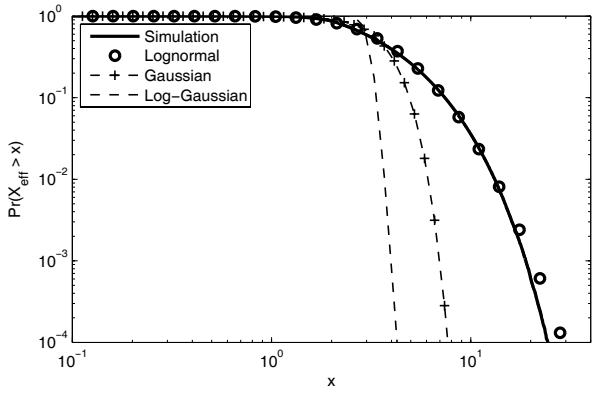

Fig. 3. Verification of the accuracy of the CCDF generated by lognormal model for EESM and comparison with other proposed distributions ($\sigma^2 = 10$ dB, $\tau = 2$, $\lambda = 1.5$, and $N = 4$).

We have also compared the accuracy of the proposed model with several other common probability distributions such as Gamma, Chi-square, Weibull, and K [35], with moment matching used to determine their parameters. These are not shown in the figure to avoid clutter. In all comparisons, the proposed model gives the best match for both CDF and CCDF. The effect of increasing the number of constituent SNRs, N, is investigated in Figure 4, which plots both the CDF and

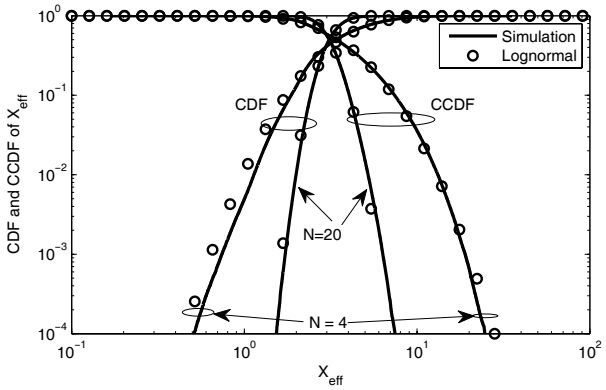

Fig. 4. Effect of the number of constituent SNRs, N, on the accuracy of the proposed statistical model for EESM ($\sigma^2 = 10$ dB, $\tau = 2$, and $\lambda = 1.5$).

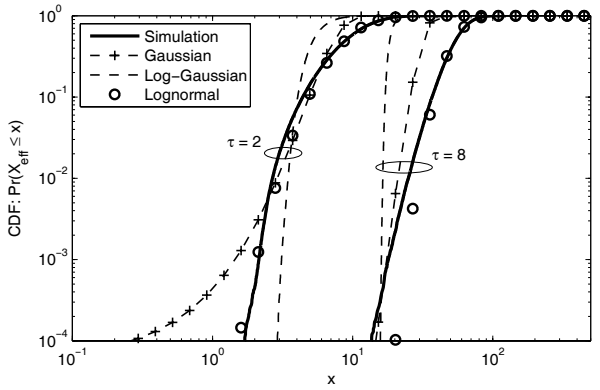

Fig. 5. Plot of the CDF of the lognormal model of EESM for different degrees of freedom, τ, which correspond to different multiple antenna modes ($\sigma^2 = 10$ dB).

TABLE I
KL DISTANCE FOR DIFFERENT DISTRIBUTIONS ($\sigma^2 = 10$ dB, $\lambda = 1.5$, $\tau = 2$, AND $N = 4$)

Probability distribution	*KL divergence*
Lognormal	0.024
Chi-square	0.052
K-distribution	0.093
Gamma	0.214
Weibull	0.403
Gaussian	3.50×10^6
Log-Gaussian	1.40×10^7

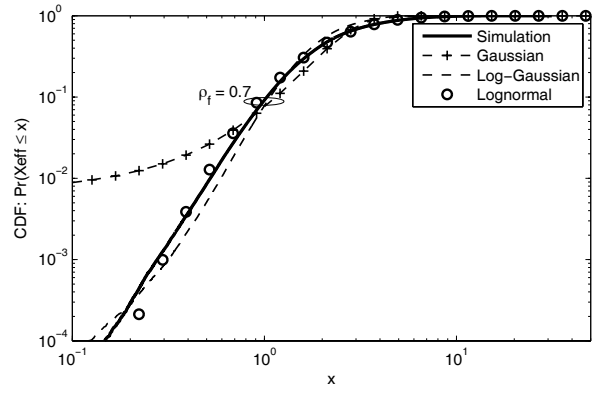

Fig. 6. Effect of frequency-domain correlation between PRBs on the accuracy of proposed lognormal model for EESM ($\sigma^2 = 10$ dB, $\tau = 4$, $\lambda = 1.5$, and $N = 4$).

CCDF. We see that the lognormal model's accuracy, in fact, increases as N increases for both the CDF and the CCDF.

The second method of comparison that quantifies the accuracy of the proposed model in a different manner is a measurement of its Kullback-Leibler (KL) divergence [36] from the empirically measured PDF. The KL divergence is a useful metric because it is zero if and only if the two distributions are identical. It is always positive, and a smaller value indicates a better match between the two distributions. The results are shown in Table I. Also tabulated are the KL divergence values for the above mentioned common distributions. We again see that the proposed lognormal model is the best one among all.

Recall that the square of a Rayleigh RV is an exponential RV, which is a Chi-square RV with $\tau = 2$ degrees of freedom. We now consider a more general case where the constituent SNRs are Chi-square RVs with $\tau \geq 2$ degrees of freedom, whose PDF is given by

$$f_{X_\tau}(x) = \frac{x^{\frac{\tau}{2}-1} e^{-\frac{x}{2}}}{2^{\frac{\tau}{2}} \Gamma\left(\frac{\tau}{2}\right)}, \quad \text{for } x \geq 0. \tag{9}$$

As we shall see, a larger τ models the effect of diversity. This can arise, for example, when multiple antenna techniques are used. Figure 5 compares the lognormal CDF with the empirical CDF of EESM for $\tau = 2$ and 8. The other parameters are kept unchanged. Again, we observe that the lognormal model characterizes the statistics of EESM well, and is considerably better than the Gaussian and log-Gaussian models. The CCDF match, which is not shown due to space constraints, is even more accurate.

The results presented thus far assumed that the PRB SNRs are uncorrelated. We now investigate the effect of correlation across PRBs on the accuracy of the proposed model. Figure 6 plots the empirical CDF of EESM and the CDF from the proposed lognormal model. Correlation between the m^{th} and n^{th} PRBs is modeled using the following geometrically decaying correlation model [12]:

$$\frac{\mathbb{E}\left[h_{n,k}(i,j) h^*_{m,k}(i,j)\right]}{\sigma_k^2} = \rho_f^{|n-m|}.$$

Results are shown for a high correlation value of $\rho_f = 0.7$. We again see that the proposed model tracks the empirical CDF of EESM well. The corresponding CCDF curves are not shown due to space constraints. We have also verified the validity of the model when the channel gains are spatially correlated or when a line-of-sight component is present. In both these cases, the PRB SNRs are no longer Chi-square RVs. The corresponding figures are again not shown due to space constraints.

Comments: Based on the CDF and CCDF matching and the KL divergence results, we find that the proposed lognormal model for EESM is accurate for a wide range of SNRs, number of constituent PRBs, and degrees of freedom (τ). It worth noting from Table I that even the Chi-square distribution comes second to the proposed model in terms of accuracy. This is an interesting observation because, at low SNRs, the

EESM can be approximated by the arithmetic mean, which has a Chi-square PDF when the PRB SNRs are i.i.d. Even when the PRB SNRs are correlated, we find the lognormal model is quite accurate even for correlations as high as $\rho_f = 0.9$.

C. Throughput Analysis of CQI Feedback Schemes

We now analyze the throughput of the UE selected subband feedback and subband-level feedback schemes. While the statistical model for EESM is a significant step forward in enabling the analysis, the following additional assumptions are made about the system model to make it analytically tractable and yet capture the interactions between the different CQI feedback techniques, EESM, scheduler, and multiple antenna diversity. We note that several of these assumptions have also been made in the related literature for analyzing relatively simpler models, and that our results are novel and significant even with these assumptions.

1) Assumptions: (i) The channel gains across different PRBs are assumed to be i.i.d. This is a valid assumption when the coherence bandwidth of the channel is close to the 180 kHz bandwidth of a PRB [1, Sec. 5.3.2]. This has also been assumed, for example, in [7], [8], [15], [22], [23], [37] to ensure analytical tractability. The channel gains are assumed to be i.i.d. across different transmit-receive antenna pairs for all UEs, which is the case when the antennas are spaced sufficiently far apart in a rich scattering environment [14], [16], [28]. This scenario has also been used in LTE performance evaluations. Thus, the gains are i.i.d. across the antenna indices l and j and across the PRB index n. However, they need not be identically distributed across the UEs since $\sigma_k^2 = \mathbb{E}\left[|h_{n,k}(l,j)|^2\right]$, which depends on the distance of the UE from the BS and shadowing, depends on k. The channel gain is assumed to remain constant over a 1 ms subframe and the feedback delays are assumed to be insignificant, which easily holds for UE speeds up to 30 kmph.

(ii) We assume that the scheduler can assign different MCSs to different PRBs that are assigned to a UE. However, in LTE, all the PRBs assigned to a UE use the same MCS. The simulation results in [38] show that the throughput difference between the two approaches is marginal.

(iii) To focus on CQI feedback, we assume ideal beamforming weight feedback for closed-loop MISO and single-stream MIMO. Clearly, no such assumption is required for SISO, SIMO, and open-loop MISO. As shown in [39], quantization of weights typically incurs a 10% loss in throughput for $N_\mathrm{r} = N_\mathrm{t} = 2$ compared to ideal feedback.

Extension to a Multi-cell Scenario: With the assumptions above, the analysis directly applies to a single cell scenario [8], [15]–[17], [23], [28], [40]. In a multi-cell scenario, the methodology can be extended by accounting for co-channel interference through its fading-averaged power. However, this extension does have its limitations since there are only six dominant first-tier interfering cells in a multi-cell OFDM system. A more sophisticated approach is pursued in [31], [41] (and references therein), which analyze cell throughput by conditioning on the fading experienced by co-channel interference. However, their models cannot be generalized to ours as they do not consider OFDM, frequency-domain scheduling, CQI feedback, and multiple antenna diversity. While [11] also conditions on the fading experienced by the co-channel interference signals and incorporates EESM, its simple cell planning oriented analysis does not consider rate adaptation, multiple antenna modes, and scheduling. Further, it uses simulations to determine the statistics of signal-to-interference-plus-noise-ratio (SINR).

2) Common Distribution for $\gamma_{n,k}$: The statistics of the SNR of n^{th} PRB of k^{th} UE, $\gamma_{n,k}$, shall play a crucial role in the analysis as the CQI depends on it. We first present a single unified characterization of the PDF of $\gamma_{n,k}$ for all the multiple antenna diversity modes, and then use it to analyze all of them together.

For SIMO ($N_\mathrm{t} = 1$, $N_\mathrm{r} \geq 2$), the receiver employs maximal-ratio combining (MRC) [27, Chap. 3]. Hence, $\gamma_{n,k} = \sum_{l=1}^{N_\mathrm{r}} |h_{n,k}(l,1)|^2$ is the summation of N_r i.i.d. exponential RVs, which is nothing but a Chi-square RV with $\tau = 2N_\mathrm{r}$ degrees of freedom and mean $N_\mathrm{r}\sigma_k^2$. Recall that $h_{n,k}(l,j)$ are i.i.d. across the transmit and receive antenna indices l and j. Clearly, SISO is a special case of SIMO with $N_\mathrm{r} = 1$. For closed-loop MISO, given the ideal beamforming weight assumption, $\gamma_{n,k} = \sum_{j=1}^{N_\mathrm{t}} |h_{n,k}(1,j)|^2$ is a Chi-square RV with $\tau = 2N_\mathrm{t}$ degrees of freedom and mean $N_\mathrm{t}\sigma_k^2$ since the transmitter employs maximal ratio transmission (MRT) for every PRB. For open-loop MISO ($N_\mathrm{t} = 2$, $N_\mathrm{r} = 1$), the Alamouti code is used. Therefore, $\gamma_{n,k}$ is again a Chi-square RV with $\tau = 2N_\mathrm{t}$ degrees of freedom and mean $N_\mathrm{t}\frac{\sigma_k^2}{2}$. Thus, for all the above multi-antenna diversity modes, we can write $\gamma_{n,k}$ as [21]

$$\gamma_{n,k} = aX_\tau + b, \tag{10}$$

where X_τ is a standard Chi-square RV with τ degrees of freedom. The values of a for SISO, SIMO, closed-loop MISO, and open-loop MISO are $\frac{\sigma_k^2}{2}$, $\frac{\sigma_k^2}{2}$, $\frac{\sigma_k^2}{2}$, and $\frac{\sigma_k^2}{4}$, respectively, and $b = 0$ for all these modes.

For single-stream MIMO ($N_\mathrm{t} = N_\mathrm{r} = 2$), $\gamma_{n,k}$ is the square of the largest singular value of the matrix $\{h_{n,k}(i,j)\}_{i,j}$ and its PDF is given as [42]

$$f_{\gamma_{n,k}}(x) = \frac{1}{\sigma_k^2}\left(\left(\frac{x}{\sigma_k^2}\right)^2 - \frac{2x}{\sigma_k^2} + 2\right)e^{-\frac{x}{\sigma_k^2}} - \frac{2}{\sigma_k^2}e^{-\frac{2x}{\sigma_k^2}},\ x \geq 0. \tag{11}$$

Its first two moments are

$$m_1 \triangleq \mathbb{E}\left[\gamma_{n,k}\right] = 3.5\sigma_k^2 \text{ and } m_2 \triangleq \mathbb{E}\left[\gamma_{n,k}^2\right] = 15.5\sigma_k^4. \tag{12}$$

While $\gamma_{n,k}$ is not a Chi-square RV, we approximate it using (10) as $aX_\tau + b$, where X_τ is a Chi-square RV with $\tau = 8$ degrees of freedom. Matching the first and second moments of $\gamma_{n,k}$ in (10) with its moments m_1 and m_2, we get $a = \sqrt{\tau\frac{m_2 - m_1^2}{2}} = 0.451\sigma_k^2$ and $b = m_1 - \tau\sqrt{\frac{m_2 - m_1^2}{2\tau}} = -0.106\sigma_k^2$. Figure 7 compares the actual and the approximate PDFs of $\gamma_{n,k}$ and verifies that the model is accurate over a wide range of values of $\gamma_{n,k}$ for single-stream MIMO.

3) Throughput of UE Selected Subband Feedback Scheme: The following two claims shall lead us to the final result for the throughput in (17). An important issue that the analysis handles is that while the CQI feedback has a coarse frequency granularity of a subband (q PRBs) or even M subbands (Mq

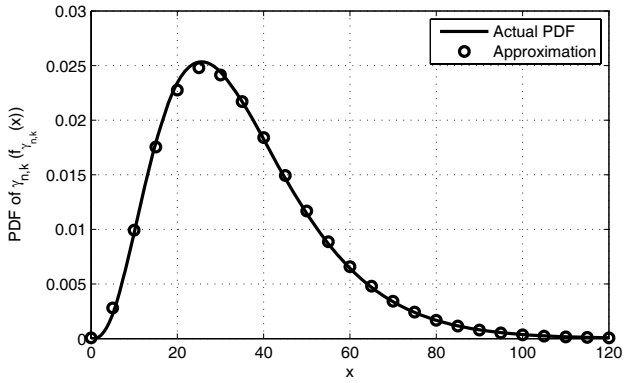

Fig. 7. Comparison of the actual PDF and approximate Chi-square PDF (with $\tau = 8$) of $\gamma_{n,k}$ for single-stream MIMO ($\sigma^2 = 10$ dB).

PRBs), the BS schedules over a narrower PRB. This can occasionally lead to an incorrect choice of the MCS.

Claim *1:* The probability that the k^{th} UE reports a CQI of r_i, for $1 \le i \le L$, is

$$\Pr\big(C_k^{\text{bestM}} = r_i\big) = \Pr\big(C_k^{\text{bestM}} \le r_i\big) - \Pr\big(C_k^{\text{bestM}} \le r_{i-1}\big), \tag{13}$$

where

$$\Pr\big(C_k^{\text{bestM}} \le r_i\big) \approx \frac{1}{\beta\Omega_k^{(Mq)}\sqrt{2\pi}} \int_0^{T_i} \frac{e^{-\frac{\left(\ln z - \mu_k^{(Mq)}\right)^2}{2\left(\Omega_k^{(Mq)}\right)^2}}}{z} \times \left(1 - 2Q\left(\frac{\ln z - \mu_k^{(q)}}{\Omega_k^{(q)}}\right)\right)^{(S-M)} dz. \tag{14}$$

Here,

$$\beta \approx \frac{1}{\sqrt{\pi}} \sum_{l=1}^{U} w_l \left(1 - 2Q\left(\frac{\sqrt{2}\Omega_k^{(Mq)}\alpha_l + \mu_k^{(Mq)} - \mu_k^{(q)}}{\Omega_k^{(q)}}\right)\right)^{(S-M)}, \tag{15}$$

and $\{w_l\}_{l=1}^U$ and $\{\alpha_l\}_{l=1}^U$ are the U Gauss-Hermite weights and abscissas, respectively [43, Tbl. 25.10]. And, $\mu_k^{(Mq)}$ and $\Omega_k^{(Mq)}$ are the lognormal parameters, as per Sec. III-A, of the EESM over the SNRs of Mq PRBs in any M subbands. An example of these SNRs is $\{\gamma_{\ell,k}\}_{\ell=1}^{Mq}$. Similarly, $\mu_k^{(q)}$ and $\Omega_k^{(q)}$ are the lognormal parameters of EESM over the SNRs of q PRBs in *any* subband. An example of these SNRs is $\{\gamma_{\ell,k}\}_{\ell=1}^{q}$.

Proof: The derivation is relegated to Appendix A. ∎

Claim *2:* Let the k^{th} UE be selected (sel.) for the n^{th} PRB and let r_i be the CQI value that it reports. Then, the conditional probability that $\gamma_{n,k}$ is less than T_{i-1} is

$$\Pr\big(\gamma_{n,k} < T_{i-1} | C_k^{\text{bestM}} = r_i, k \text{ is sel. for } n^{\text{th}} \text{ PRB}\big) \approx \frac{1}{Q\left(\frac{\ln T_{i-1} - \mu_k^{(Mq)}}{\Omega_k^{(Mq)}}\right) - Q\left(\frac{\ln T_i - \mu_k^{(Mq)}}{\Omega_k^{(Mq)}}\right)} \int_{-\frac{b}{a}}^{\frac{T_{i-1}-b}{a}} \frac{y^{\frac{\tau}{2}-1}e^{-\frac{y}{2}}}{2^{\frac{\tau}{2}}\left(\frac{\tau}{2}-1\right)!} \times \left[Q\left(\frac{\ln\left[-\lambda \ln\left(\frac{Mqe^{-\frac{\zeta_M(T_{i-1},\frac{y-b}{a})}{\lambda}} - e^{-\frac{y-b}{a\lambda}}}{Mq-1}\right)\right] - \mu_k^{(Mq-1)}}{\Omega_k^{(Mq-1)}}\right) - Q\left(\frac{\ln\left[-\lambda \ln\left(\frac{Mqe^{-\frac{\zeta_M(T_i,\frac{y-b}{a})}{\lambda}} - e^{-\frac{y-b}{a\lambda}}}{Mq-1}\right)\right] - \mu_k^{(Mq-1)}}{\Omega_k^{(Mq-1)}}\right)\right] dy,$$

where

$$\zeta_\ell(x,y) = \min\left\{\max\left\{-\lambda \ln\left(\frac{\ell q - 1 + e^{-\frac{y}{\lambda}}}{\ell q}\right), x\right\}, y + \lambda \ln(\ell q)\right\}, \quad \text{for } l = 1, 2, \ldots. \tag{16}$$

As used in Claim 1, $\mu_k^{(Mq)}$ and $\Omega_k^{(Mq)}$ are the lognormal parameters of EESM over any Mq PRBs. And, $\mu_k^{(Mq-1)}$ and $\Omega_k^{(Mq-1)}$ are the lognormal parameters of EESM over the SNRs $\gamma_{1,k}, \gamma_{2,k}, \ldots, \gamma_{Mq-1,k}$.

Proof: The proof is relegated to Appendix B. ∎

Using the above results, the throughput of the PF scheduler, which is defined in (4), is as follows.

Result *1:* The average throughput, $\bar{R}_n$, for PRB n is

$$\bar{R}_n = \sum_{\mathcal{Z}_{s(n)}} \Pr\big(\mathcal{Z}_{s(n)}\big) \sum_{k \in \mathcal{Z}_{s(n)}} \sum_{i=1}^{L} r_i \Pr\big(C_k^{\text{bestM}} = r_i\big) \times \big(1 - \Pr\big(\gamma_{n,k} < T_{i-1} | C_k^{\text{bestM}} = r_i, k \text{ is sel. for } n^{\text{th}} \text{ PRB}\big)\big) \times \left[\prod_{l \in \mathcal{Z}_{s(n)},\ l \ne k} \Pr\big(C_l^{\text{bestM}} \le \vartheta_{l,i}\big)\right]. \tag{17}$$

where $\vartheta_{l,i}$ is the largest rate that is strictly less than $\frac{\mathbb{E}\left[C_l^{\text{bestM}}\right]}{\mathbb{E}\left[C_k^{\text{bestM}}\right]} r_i$, $\Pr\big(C_l^{\text{bestM}} \le \vartheta_{l,i}\big)$ is given by Claim 1, $\Pr\big(\gamma_{n,k} < T_{i-1} | C_k^{\text{bestM}} = r_i, k \text{ is sel. for } n^{\text{th}} \text{ PRB}\big)$ is given in Claim 2, and $\Pr\big(\mathcal{Z}_{s(n)}\big) = \left(\frac{M}{S}\right)^{|\mathcal{Z}_{s(n)}|} \left(1 - \frac{M}{S}\right)^{K - |\mathcal{Z}_{s(n)}|}$.

Proof: The proof is given in Appendix C. ∎

The above throughput expression is in the form of a single integral, which is numerically evaluated. This is a significant simplification compared to either brute-force simulations or an N-fold integral with a considerably more involved integrand that would arise if the proposed lognormal model is not used for EESM.

4) Throughput of Subband-Level Feedback Scheme: The following claim shall lead us to the final expression for the throughput in (20).

Claim *3:* Let the k^{th} UE be selected for the n^{th} PRB and the CQI value reported by it be r_i. The probability of an outage, *i.e.*, $\gamma_{n,k} \le T_{i-1}$, is

$$\Pr\Big(\gamma_{n,k} < T_{i-1} | C_{s(n),k}^{\text{sub}} = r_i, k \text{ is sel. for } n^{\text{th}} \text{ PRB}\Big) = \frac{1}{\Pr\left(C_{s(n),k}^{\text{sub}} = r_i\right)} \int_{-\frac{b}{a}}^{\frac{T_{i-1}-b}{a}} \frac{y^{\frac{\tau}{2}-1}e^{-\frac{y}{2}}}{2^{\frac{\tau}{2}}\left(\frac{\tau}{2}-1\right)!} \times \left[Q\left(\frac{\ln\left[-\lambda \ln\left(\frac{qe^{-\frac{\zeta_1\left(T_{i-1},\frac{y-b}{a}\right)}{\lambda}} - e^{-\frac{y-b}{a\lambda}}}{q-1}\right)\right] - \mu_k^{(q-1)}}{\Omega_k^{(q-1)}}\right)\right.$$

$$-Q\left(\frac{\ln\left[-\lambda\ln\left(\frac{qe^{-\frac{\zeta_1\left(T_i,\frac{y-b}{a}\right)}{\lambda}}-e^{-\frac{y-b}{a\lambda}}}{q-1}\right)\right]-\mu_k^{(q-1)}}{\Omega_k^{(q-1)}}\right)dy, \tag{18}$$

where

$$\Pr\left(C_{s(n),k}^{\text{sub}}=r_i\right)=Q\left(\frac{\ln\left(T_{i-1}\right)-\mu_k^{(q)}}{\Omega_k^{(q)}}\right)-Q\left(\frac{\ln\left(T_i\right)-\mu_k^{(q)}}{\Omega_k^{(q)}}\right), \tag{19}$$

and $\zeta_1(x,y)$ is defined in Claim 2. Here, $\mu_k^{(q)}$ and $\Omega_k^{(q)}$, as already used in Claim 1, are the lognormal parameters of EESM over the SNRs of all the q PRBs of a subband for the k^{th} UE. And, $\mu_k^{(q-1)}$ and $\Omega_k^{(q-1)}$ are the lognormal parameters of EESM over the SNRs of any $q-1$ PRBs in a subband of the k^{th} UE, e.g., $\{\gamma_{\ell,k}\}_{\ell=1}^{q-1}$.

Proof: The proof is similar to that in Appendix B and is omitted to conserve space. ∎

Result *2:* The average throughput, $\bar{R}_n$, for PRB n of the subband-level CQI feedback scheme is

$$\bar{R}_n=\sum_{k=1}^{K}\sum_{i=1}^{L}r_i\Pr\left(C_{s(n),k}^{\text{sub}}=r_i\right)\left[\prod_{l=1,l\neq k}^{K}\Pr\left(C_{s(n),l}^{\text{sub}}\leq\vartheta_{l,i}\right)\right]\times\left(1-\Pr\left(\gamma_{n,k}<T_{i-1}|C_{s(n),k}^{\text{sub}}=r_i,k\text{ is sel. for }n^{\text{th}}\text{ PRB}\right)\right), \tag{20}$$

where $\vartheta_{l,i}$ is the largest rate among $\{r_1,\ldots,r_L\}$ that is strictly less than $\frac{\mathbb{E}\left[C_{s(n),l}^{\text{sub}}\right]}{\mathbb{E}\left[C_{s(n),k}^{\text{sub}}\right]}r_i$, and $\Pr\left(C_{s(n),k}^{\text{sub}}=r_i\right)$ and $\Pr\left(\gamma_{n,k}<T_{i-1}|C_{s(n),k}^{\text{sub}}=r_i,k\text{ is sel. for }n^{\text{th}}\text{ PRB}\right)$ are given in Claim 3.

Proof: The proof is relegated to Appendix D. ∎

As before, the final result is in the form of a single integral, which is numerically evaluated.

IV. LTE Throughput Results And Comparisons

We now use Monte Carlo simulations that average over 50,000 samples to verify the analysis. We consider a single cell with $K=6$ UEs in it and a BS at the center of the cell. As discussed in Section II, the channel gains of the PRBs for different transmit-receive antenna pairs for the k^{th} UE are generated as independent zero-mean complex Gaussian RVs with variance σ_k^2 . To model the non-i.i.d. channels seen by different UEs, we set $\sigma_k^2=\lambda/\alpha^{k-1}$, $1\leq k\leq K$, where $\alpha\geq 1$. Effectively, the first UE sees the strongest channel (on average) and UEs $2,\ldots,K$ see successively weaker channels (on average).

The set of link adaptation thresholds are generated using the coding gain loss model of [44]. They are related to the rate as follows: $r_i=\log_2\left(1+\zeta T_{i-1}\right)$. Here, ζ is the coding gain loss, and is set as $\zeta=0.398$ as per [44]. A smaller value of ζ means a lower (tighter) bit error constraint. Note that our analysis applies to any set of adaptation thresholds $T_0,\ldots,T_L$.

TABLE II
LOGNORMAL PARAMETERS OF EESM ($\sigma^2=10$ DB AND $\lambda=1.5$)

Degrees of freedom τ	*Number of subcarriers*	*Lognormal parameters*	
		μ	Ω
2	3	1.35	0.40
	4	1.26	0.30
	11	1.16	0.09
	12	1.16	0.08
4	3	2.26	0.27
	4	2.19	0.22
	11	1.96	1.11
	12	1.94	0.10
8	3	3.19	0.14
	4	3.09	0.14
	11	2.87	0.08
	12	2.25	0.08

The thresholds can alternately be chosen based on link-level simulation results.

A subband consists of $q=4$ PRBs. The number of subbands is $S=6$, which corresponds to a cell bandwidth of $B=5$ MHz. In the UE selected subband feedback scheme, each UE selects $M=3$ out of $S=6$ subbands. Unless mentioned otherwise, $\rho=10$ dB, $\alpha=1.2$, and $\lambda=1.5$. Since we are using the lognormal model of EESM, the lognormal parameters of EESM are computed once in the analysis. For example, Table II enumerates these parameters for the 1st UE for different τ. Since the throughput for SIMO and closed-loop MISO are the same given σ_k^2, we show results only for the former.

Figure 8 plots the average throughput as a function of K for the UE selected subband scheme. This is done for SISO, SIMO ($N_{\text{r}}=2$), open-loop MISO ($N_{\text{t}}=2$), and single-stream MIMO. The throughput decreases marginally once K exceeds 4. This is because the PF scheduler ensures fairness among the UEs even though the additional UEs have lower average SNRs. A similar effect is observed for the subband-level feedback scheme. The throughput of single-stream MIMO, SIMO, and open-loop MISO is 140%, 70%, and 10% more than SISO, respectively. We see that the analysis and simulation results differ by no more than 8%. The difference occurs because of the lognormal approximation of EESM and the approximation in Claim 1.

To compare the two CQI feedback schemes, Figure 9 plots their average throughput (from analysis) for SISO, SIMO, and single-stream MIMO. As the number of UEs increases, the throughput of the UE selected subband scheme approaches that of the subband-level feedback scheme for all the multiple antenna modes despite its lower feedback overhead.

Figure 10 plots the throughput of UE selected subband feedback (from analysis) for different values of M and q for SISO. When M is small, the throughput increases as M increases since the CQI is reported for more subbands. However, for larger M, the throughput decreases since the UE feeds back only one CQI value for all M subbands. Further, for the same M, a larger q always leads to a lower throughput since the subband-level CQI is an average of more PRBs. We see that for $q=2$, the optimum M is 2, while for $q=4$, the optimum M is 3.

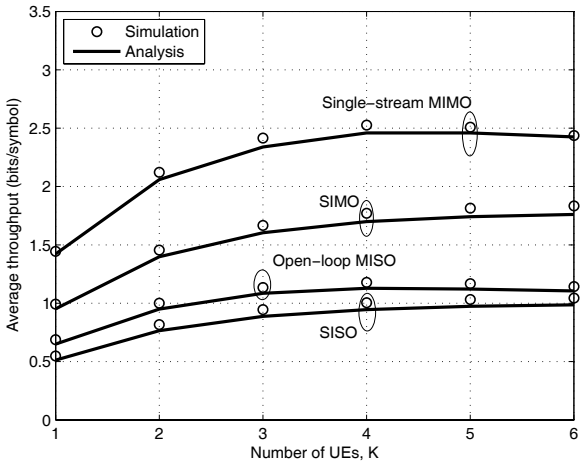

Fig. 8. Comparison of the average throughput of UE selected subband feedback scheme from analysis and simulations for different multiple antenna modes.

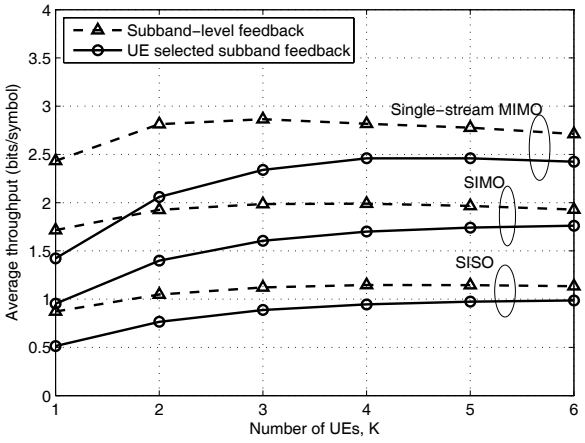

Fig. 9. Comparison of the average throughputs of UE selected subband feedback and subband-level feedback schemes (from analysis) for different numbers of UEs, K.

V. Conclusions

EESM is an empirical tool that is widely used in the design, analysis, and simulation of OFDM and OFDM systems. However, an analysis of systems that use EESM has been hampered by the highly non-linear nature of EESM. Even a closed-form probability distribution function for the effective SNR is unknown. We developed an analytically tractable model for EESM that empirically models it as a lognormal RV, and showed that the model is accurate under a variety of scenarios. We verified its accuracy when the PRBs channel gains are uncorrelated or correlated, and in the presence of frequency-domain correlation and spatial-domain correlation.

The lognormal model of EESM was then instrumental in developing an accurate analysis for the throughput of the UE selected subband CQI feedback and subband-level CQI feedback schemes of LTE. In both these schemes, EESM is used to determine the CQI, which is averaged over many PRBs to reduce the feedback overhead. The analysis captured the joint effect of multi-antenna diversity mode, scheduler, CQI feedback scheme, and CQI generation. The throughput expressions were in the form of single integrals, which is a significant advance compared to the brute-force simulations that have typically been used to study this problem. It also enabled the optimization of the CQI feedback scheme's parameters.While the analysis does not obviate the need for detailed system-level simulations, it provides a valuable, independent and common theoretical reference to an LTE system designer. It enables the designer to quickly optimize parameters, gain intuition, and saves considerable simulation effort.

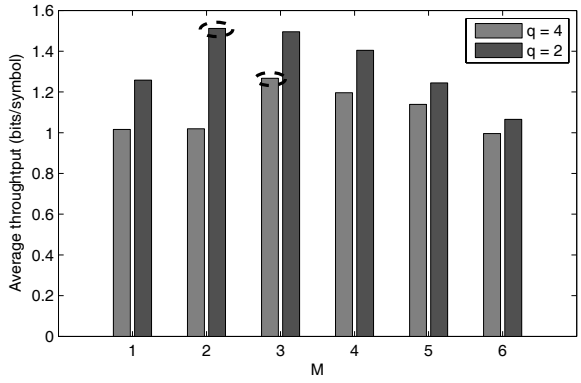

Fig. 10. Optimization of parameters of the UE selected subband feedback scheme as a function of the number of PRBs in a subband, q. The bars corresponding to the optimal values of M are encircled.

Appendix

A. Proof of Claim 1

From Sec. II-B1, $\Pr\big(C_k^{\text{bestM}} \le r_i\big) = \Pr\big(\gamma_k^{\text{rep}} < T_i\big)$. To evaluate this probability, we need the PDF of the EESM of M *ordered* subband effective SNRs, which is analytically intractable. We circumvent this problem by deriving an approximate expression that involves only a single integral as follows [21]:

$$\begin{aligned}\Pr\big(\gamma_k^{\text{rep}} < T_i\big) &\overset{\text{(i)}}{=} \sum_{i_1,\ldots,i_M} \Pr\big(\gamma_k^{\text{rep}} < T_i, \mathcal{I}_k = \{i_1,\ldots,i_M\}\big) \\ &\overset{\text{(ii)}}{=} \binom{S}{M} \Pr\big(\gamma_k^{\text{rep}} < T_i, \mathcal{I}_k = \{1,\ldots,M\}\big).\end{aligned} \tag{21}$$

Here, (i) follows from the law of total probability. Since for a given UE, the subband SNRs are i.i.d. and there are $\binom{S}{M}$ possible combinations of best M subbands, we get (ii).

Let Λ be the event $\mathcal{I}_k = \{1,\ldots,M\}$. Then,

$$\Pr(\Lambda) = \Pr\Big(\max_{M+1\le l\le S}\big(\gamma_{l,k}^{\text{sub}}\big) \le \min\big(\gamma_{1,k}^{\text{sub}},\ldots,\gamma_{M,k}^{\text{sub}}\big)\Big). \tag{22}$$

From [10], we know that

$$\min\big(\gamma_{1,k}^{\text{sub}},\ldots,\gamma_{M,k}^{\text{sub}}\big) \le \gamma_k^{\text{rep}} = -\lambda \ln\left(\frac{1}{M}\sum_{i=1}^{M} e^{-\frac{\gamma_{i,k}^{\text{sub}}}{\lambda}}\right).$$

We then get

$$\Pr(\Lambda) \le \Pr\left(\max_{M+1\le l\le S}\big(\gamma_{l,k}^{\text{sub}}\big) \le \gamma_k^{\text{rep}}\right). \tag{23}$$

Thus, from (21),

$$\Pr\big(C_k^{\text{bestM}} \le r_i\big) \le \binom{S}{M}\Pr\left(\max_{M+1\le l\le S}\left(\gamma_{l,k}^{\text{sub}}\right) \le \gamma_k^{\text{rep}} < T_i\right), \quad (24)$$

$$= \binom{S}{M}\int_0^{T_i} f_{\gamma_k^{\text{rep}}}(z)\left(\Pr\big(\gamma_{M+1,k}^{\text{sub}} \le z\big)\right)^{(S-M)} dz. \quad (25)$$

At the same time, we know that $\Pr\big(C_k^{\text{bestM}} \le r_L\big) = 1$, since r_L is the highest rate. This motivates the following approximation that, by design, is exact for $i = L$. In it, the upper bound in (25) is divided by a factor $\binom{S}{M}\beta$, where β is the probability that $C_k^{\text{bestM}} = r_L$. Using the proposed lognormal approximation (Sec. III-A), we know that $\gamma_k^{\text{rep}} = -\lambda \ln\left(\frac{1}{M}\sum_{i=1}^{M} e^{-\frac{\gamma_{i,k}^{\text{sub}}}{\lambda}}\right)$, which is the EESM computed over Mq PRB SNRs, is a lognormal RV with parameters $\mu_k^{(Mq)}$ and $\Omega_k^{(Mq)}$. Similarly, $\gamma_{M+1,k}^{\text{sub}}$ is a lognormal RV with parameters $\mu_k^{(q)}$ and $\Omega_k^{(q)}$. Therefore,

$$\beta = \int_{-\infty}^{\infty} \frac{e^{-\frac{\left(z-\mu_k^{(Mq)}\right)^2}{2\left(\Omega_k^{(Mq)}\right)^2}}}{\Omega_k^{(Mq)}\sqrt{2\pi}}\left(1 - Q\left(\frac{z-\mu_k^{(q)}}{\Omega_k^{(q)}}\right)\right)^{(S-M)} dz. \quad (26)$$

Applying Gauss-Hermite quadrature [43] to (26) results in the desired expression for β.

B. Proof of Claim 2

For brevity, let

$$\psi_k = \Pr\big(\gamma_{n,k} < T_{i-1} | C_k^{\text{bestM}} = r_i, k \text{ is sel. for } n^{\text{th}} \text{ PRB}\big). \quad (27)$$

Applying a method similar to the one used in Appendix A results in a three-fold integral expression for ψ_k that cannot be simplified further. Hence, we develop a different method below, which leads to a much simpler single-fold integral expression.

From Baye's rule and (4), we get

$$\psi_k = \frac{\Pr\left(\gamma_{n,k} < T_{i-1}, C_k^{\text{bestM}} = r_i, \frac{C_l^{\text{bestM}}}{\mathbb{E}\left[C_l^{\text{bestM}}\right]} < \frac{r_i}{\mathbb{E}\left[C_k^{\text{bestM}}\right]}, \forall\, l \ne k\right)}{\Pr\left(C_k^{\text{bestM}} = r_i, \frac{C_l^{\text{bestM}}}{\mathbb{E}\left[C_l^{\text{bestM}}\right]} < \frac{r_i}{\mathbb{E}\left[C_k^{\text{bestM}}\right]}, \forall\, l \ne k\right)}.$$

Since the CQIs fed back by different UEs are mutually independent, the above expression simplifies to

$$\psi_k = \frac{\Pr\big(\gamma_{n,k} < T_{i-1}, C_k^{\text{bestM}} = r_i,\big)}{\Pr\big(C_k^{\text{bestM}} = r_i\big)}. \quad (28)$$

Further, $C_k^{\text{bestM}} = r_i$ if and only if the EESM of the subband SNRs in $\mathcal{I}_k$, $\gamma_k^{\text{rep}} = -\lambda \ln\left(\frac{1}{M}\sum_{v\in\mathcal{I}_k} e^{-\frac{\gamma_{v,k}^{\text{sub}}}{\lambda}}\right)$, lies in between T_{i-1} and T_i. Hence,

$$\psi_k = \frac{\Pr\left(\gamma_{n,k} < T_{i-1}, T_{i-1} \le -\lambda \ln\left(\frac{1}{M}\sum_{v\in\mathcal{I}_k} e^{-\frac{\gamma_{v,k}^{\text{sub}}}{\lambda}}\right) < T_i\right)}{\Pr\left(T_{i-1} \le -\lambda \ln\left(\frac{1}{M}\sum_{v\in\mathcal{I}_k} e^{-\frac{\gamma_{v,k}^{\text{sub}}}{\lambda}}\right) < T_i\right)}. \quad (29)$$

Note that the set $\mathcal{I}_k$ contains the subband $s(n)$.

Without loss of generality, since the PRB SNRs and the subband effective SNRs are i.i.d., let $n = 1$, $s(1) = 1$, and $\mathcal{I}_k = \{1, \ldots, M\}$. Since $\binom{S-1}{M-1}$ sets of M subbands contain subband 1, the numerator of (29) is $\binom{S-1}{M-1}\Pr\left(\gamma_{1,k} < T_{i-1}, T_{i-1} \le -\lambda \ln\left(\frac{1}{M}\sum_{v\in\mathcal{I}_k} e^{-\frac{\gamma_{v,k}^{\text{sub}}}{\lambda}}\right) < T_i, \mathcal{I}_k = \{1, \ldots, M\}\right)$. Similarly, the denominator of (29) is

$$\binom{S-1}{M-1}\Pr\left(T_{i-1} \le -\lambda \ln\left(\frac{1}{M}\sum_{v\in\mathcal{I}_k} e^{-\frac{\gamma_{v,k}^{\text{sub}}}{\lambda}}\right) < T_i, \mathcal{I}_k = \{1, \ldots, M\}\right).$$

Substituting these in (29) and using Baye's rule yields

$$\psi_k = \frac{\Pr\left(\begin{matrix}\mathcal{I}_k = \{1,\ldots,M\} | \gamma_{1,k} < T_{i-1}, T_{i-1} \le \\ -\lambda \ln\left(\frac{1}{M}\sum_{v=1}^{M} e^{-\frac{\gamma_{v,k}^{\text{sub}}}{\lambda}}\right) < T_i\end{matrix}\right)}{\Pr\left(\begin{matrix}\mathcal{I}_k = \{1,\ldots,M\} | T_{i-1} \le \\ -\lambda \ln\left(\frac{1}{M}\sum_{v=1}^{M} e^{-\frac{\gamma_{v,k}^{\text{sub}}}{\lambda}}\right) < T_i\end{matrix}\right)} \times \frac{\Pr\left(\gamma_{1,k} < T_{i-1}, T_{i-1} \le -\lambda \ln\left(\frac{1}{M}\sum_{v=1}^{M} e^{-\frac{\gamma_{v,k}^{\text{sub}}}{\lambda}}\right) < T_i\right)}{\Pr\left(T_{i-1} \le -\lambda \ln\left(\frac{1}{M}\sum_{v=1}^{M} e^{-\frac{\gamma_{v,k}^{\text{sub}}}{\lambda}}\right) < T_i\right)}. \quad (30)$$

We observe that the event $\mathcal{I}_k = \{1, \ldots, M\}$ is weakly dependent on the event $\gamma_{1,k} < T_{i-1}$. This is because the event $\gamma_{1,k} < T_{i-1}$ primarily affects the probability that subband 1 is selected. Further, $Mq - 1$ other PRBs also affect $\mathcal{I}_k$. Neglecting $\gamma_{1,k} < T_{i-1}$ in the numerator and simplifying gives

$$\psi_k \approx \frac{\Pr\left(\gamma_{1,k} < T_{i-1}, T_{i-1} \le -\lambda \ln\left(\frac{1}{M}\sum_{v=1}^{M} e^{-\frac{\gamma_{v,k}^{\text{sub}}}{\lambda}}\right) < T_i\right)}{\Pr\left(T_{i-1} \le -\lambda \ln\left(\frac{1}{M}\sum_{v=1}^{M} e^{-\frac{\gamma_{v,k}^{\text{sub}}}{\lambda}}\right) < T_i\right)}. \quad (31)$$

From (2) and (3), we have $-\lambda \ln\left(\frac{1}{M}\sum_{v=1}^{M} e^{-\frac{\gamma_{v,k}^{\text{sub}}}{\lambda}}\right) = -\lambda \ln\left(\frac{1}{Mq}\sum_{v=2}^{Mq} e^{-\frac{\gamma_{v,k}}{\lambda}} + \frac{e^{-\frac{\gamma_{1,k}}{\lambda}}}{Mq}\right)$, which is the EESM of Mq PRB SNRs, one of which is $\gamma_{1,k}$. Further, from (10), $\gamma_{1,k} = aX_\tau + b$, where a, b, and τ depend on the multiple antenna mode. Upon writing the numerator of (31) in terms of PDF of the Chi-square RV X_τ (given in (9)), we get

$$\Pr\left(\begin{matrix}\gamma_{1,k} < T_{i-1}, T_{i-1} \le \\ -\lambda \ln\left(\frac{1}{Mq}\sum_{v=1}^{Mq-1} e^{-\frac{\gamma_{v,k}}{\lambda}} + \frac{e^{-\frac{aX_\tau+b}{\lambda}}}{Mq}\right) < T_i\end{matrix}\right) = \int_{-\frac{b}{a}}^{\frac{T_{i-1}-b}{a}} \frac{y^{\frac{\tau}{2}-1}e^{-\frac{y}{2}}}{(2)^{\frac{\tau}{2}}\left(\frac{\tau}{2}-1\right)!}\Pr\left(\zeta_M\left(T_{i-1}, \frac{y-b}{a}\right) \le -\lambda \ln\left(\frac{1}{Mq}\sum_{v=1}^{Mq-1} e^{-\frac{\gamma_{v,k}}{\lambda}} + \frac{e^{-\frac{y-b}{a\lambda}}}{Mq}\right) < \zeta_M(T_i, y)\right) dy,$$

where $\zeta_M(\cdot,\cdot)$ is given in the claim statement. It follows because, given that $\gamma_{n,k} = y$, the term

$-\lambda \ln\left(\frac{1}{Mq}\sum_{v=1}^{Mq-1} e^{-\frac{\gamma_{v,k}}{\lambda}} + \frac{e^{-\frac{y}{\lambda}}}{Mq}\right)$ must lie between $-\lambda \ln\left(\frac{Mq-1+e^{-\frac{y-b}{a\lambda}}}{Mq}\right)$ and $\frac{y-b}{a} + \lambda \ln(Mq)$.

Rearranging the terms and opening up the integrand in the numerator, simplifies the numerator to

$$\int_{-\frac{b}{a}}^{\frac{T_{i-1}-b}{a}} \frac{y^{\frac{\tau}{2}-1}e^{-\frac{y}{2}}}{(2)^{\frac{\tau}{2}}\left(\frac{\tau}{2}-1\right)!} \times \left[\Pr\left(\begin{array}{c}-\lambda \ln\left(\frac{1}{Mq-1}\sum_{v=1}^{Mq-1} e^{-\frac{\gamma_{v,k}}{\lambda}}\right) < \\ -\lambda \ln\left(\frac{Mqe^{-\frac{\zeta_M(T_i,\frac{y-b}{a})}{\lambda}} - e^{-\frac{y-b}{a\lambda}}}{Mq-1}\right)\end{array}\right) - \Pr\left(\begin{array}{c}-\lambda \ln\left(\frac{1}{Mq-1}\sum_{v=1}^{Mq-1} e^{-\frac{\gamma_{v,k}}{\lambda}}\right) \leq \\ -\lambda \ln\left(\frac{Mqe^{-\frac{\zeta_M(T_{i-1},\frac{y-b}{a})}{\lambda}} - e^{-\frac{y-b}{a\lambda}}}{Mq-1}\right)\end{array}\right)\right] dy.$$

The above two probabilities can be written in terms of the Gaussian $Q(.)$ function since $-\lambda \ln\left(\frac{1}{Mq-1}\sum_{v=1}^{Mq-1} e^{-\frac{\gamma_{v,k}}{\lambda}}\right)$, which is the effective SNR over $Mq-1$ PRB SNRs, is a lognormal RV with parameters $\mu_k^{(Mq-1)}$ and $\Omega_k^{(Mq-1)}$. Similarly, we use the lognormal model for EESM to simplify the denominator of (31) as well. Combining these gives the required result.

C. Proof of Result 1

Since the SNRs of different PRBs of a UE are i.i.d., the probability that a UE selects the subband $s(n)$ is $\frac{M}{S}$. Hence, $\Pr\left(\mathcal{Z}_{s(n)}\right) = \left(\frac{M}{S}\right)^{|\mathcal{Z}_{s(n)}|}\left(1-\frac{M}{S}\right)^{\left(K-|\mathcal{Z}_{s(n)}|\right)}$. A rate r_i is achieved if the UE that is selected for the PRB fed back a CQI value equal to r_i and there was no outage. The probability that the k^{th} UE gets selected, given that it fed back the rate r_i, is $\prod_{\substack{l\in\mathcal{Z}_{s(n)}\\ l\neq k}} \Pr\left(C_l^{\text{bestM}} \leq \vartheta_{l,i}\right)$. This is because the k^{th} UE is selected only if $C_l^{\text{bestM}} < \frac{\mathbb{E}\left[C_l^{\text{bestM}}\right]}{\mathbb{E}\left[C_k^{\text{bestM}}\right]} r_i$, for $l \neq k$.[8] The law of total expectation then yields (17).

D. Proof of Result 2

A rate r_i is achieved if the UE, say the k^{th} UE, that is selected for the PRB fed back a CQI value equal to r_i and there was no outage. This results in the expression for the average throughput in (20), where the probability that the k^{th} UE gets selected given that it fed back the rate r_i is $\prod_{\substack{l=1\\ l\neq k}}^{K} \Pr\left(C_{s(n),l}^{\text{sub}} \leq \vartheta_{l,i}\right)$. This is because the k^{th} UE is selected only if $C_{s(n),l}^{\text{sub}} < \frac{\mathbb{E}\left[C_{s(n),l}^{\text{sub}}\right]}{\mathbb{E}\left[C_{s(n),k}^{\text{sub}}\right]} r_i$, for all $l \neq k$.

ACKNOWLEDGMENTS

We thank the editor and the anonymous reviewers for their comments, which helped improve the presentation of this paper.

[8]The equality case $C_l^{\text{bestM}} = \frac{\mathbb{E}\left[C_l^{\text{bestM}}\right]}{\mathbb{E}\left[C_k^{\text{bestM}}\right]} r_i$ need not be considered as it occurs with zero probability in a random deployment of UEs.

REFERENCES

[1] S. Sesia, I. Toufik, and M. Baker, *LTE–The UMTS Long Term Evolution, From Theory to Practice*. John Wiley and Sons, 2009.

[2] S. T. Chung and A. J. Goldsmith, "Degrees of freedom in adaptive modulation: a unified view," *IEEE Trans. Commun.*, vol. 49, pp. 1561–1571, Jan. 2001.

[3] M. Pauli, U. Wachsmann, and S. Tsai, "Quality determination for a wireless communications link." U.S. Patent Office publication, Patent US 2004/0219883, Nov. 2004.

[4] E. Westman, "Calibration and evaluation of the exponential effective SINR mapping (EESM) in 802.16," Master's thesis, The Royal Institute of Technology (KTH), Stockholm, Sweden, Sep. 2006.

[5] E. Tuomaala and H. Wang, "Effective SINR approach of link to system mapping in OFDM/multi-carrier mobile network," in *Proc. Int. Conf. Mobile Tech., Appl. Syst.*, Nov. 2005.

[6] "Feasibility study for OFDM for UTRAN enhancement," Tech. Rep. 25.892 v6.0.0 (2004-06), 3rd Generation Partnership Project (3GPP).

[7] S. Sanayei and A. Nosratinia, "Opportunistic downlink transmission with limited feedback," *IEEE Trans. Inf. Theory*, vol. 53, pp. 4363–4372, Nov. 2007.

[8] J. Chen, R. A. Berry, and M. L. Honig, "Limited feedback schemes for downlink OFDMA based on sub-channel groups," *IEEE J. Sel. Areas Commun.*, vol. 26, pp. 1451–1461, Oct. 2008.

[9] K. I. Pedersen, G. Monghal, I. Z. Kovács, T. E. Kolding, A. Pokhariyal, F. Frederiksen, and P. Mogensen, "Frequency domain scheduling for OFDMA with limited and noisy channel feedback," in *Proc. VTC (Fall)*, pp. 1792–1796, Oct. 2007.

[10] H. Song, R. Kwan, and J. Zhang, "General results on SNR statistics involving EESM-based frequency selective feedbacks," *IEEE Trans. Wireless Commun.*, vol. 9, pp. 1790–1798, May 2010.

[11] R. Giuliano and F. Mazzenga, "Exponential effective SINR approximations for OFDM/OFDMA-based cellular system planning," *IEEE Trans. Wireless Commun.*, vol. 8, pp. 4434–4439, Sep. 2009.

[12] R. Kwan, C. Leung, and J. Zhang, "Proportional fair multiuser scheduling in LTE," *IEEE Signal Process. Lett.*, vol. 16, pp. 461–464, June 2009.

[13] A. Pokhariyal, T. E. Kolding, and P. E. Mogensen, "Performance of downlink frequency domain packet scheduling for the UTRAN Long Term Evolution," in *Proc. PIMRC*, Sep. 2006.

[14] E. Dahlman, H. Ekstrom, A. Furuskar, Y. Jading, J. Karlsson, M. Lundevall, and S. Parkvall, "The 3G Long-Term-Evolution radio interface concepts and performance evaluation," in *Proc. VTC (Spring)*, pp. 137–141, May 2006.

[15] J. Leinonen, J. Hamalainen, and M. Juntti, "Performance analysis of downlink OFDMA resource allocation with limited feedback," *IEEE Trans. Veh. Technol.*, vol. 8, pp. 2927–2937, June 2009.

[16] S. Catreux, P. F. Driessen, and L. J. Greenstein, "Data throughputs using multiple-input multiple-output (MIMO) techniques in a noise-limited cellular environment," *IEEE Trans. Wireless Commun.*, vol. 1, pp. 226–235, Apr. 2002.

[17] M. Torabi, D. Haccoun, and W. Ajib, "Performance analysis of scheduling schemes for rate-adaptive MIMO OSFBC-OFDM systems," *IEEE Trans. Veh. Technol.*, vol. 59, pp. 2363–2379, June 2010.

[18] P. Svedman, S. K. Wilson, L. J. Cimimi, and B. Ottersten, "Opportunistic beamforming and scheduling for OFDMA systems," *IEEE Trans. Commun.*, vol. 55, pp. 941–952, May 2007.

[19] S. N. Donthi and N. B. Mehta, "Performance analysis of user selected subband channel quality indicator feedback scheme of LTE," in *Proc. IEEE Globecom*, Dec. 2010.

[20] S. N. Donthi and N. B. Mehta, "Performance analysis of subband-level channel quality indicator feedback scheme of LTE," in *Proc. Nat. Conf. Commun.*, Jan. 2010.

[21] S. N. Donthi and N. B. Mehta, "Performance analysis of channel quality indicator feedback schemes of LTE," to appear in *IEEE Trans. Veh. Technol.*, 2011.

[22] Z. Lin, P. Xiao, and B. Vucetic, "SINR distribution for LTE downlink multiuser MIMO systems," in *Proc. ICASSP*, pp. 2833–2836, Apr. 2009.

[23] S. Ko, S. Lee, H. Kwon, and B. G. Lee, "Mode selection-based channel feedback reduction schemes for opportunistic scheduling in OFDMA systems," *IEEE Trans. Wireless Commun.*, vol. 9, pp. 2842–2852, Sep. 2010.

[24] N. B. Mehta, J. Wu, A. F. Molisch, and J. Zhang, "Approximating a sum of random variables with a lognormal," *IEEE Trans. Wireless Commun.*, vol. 6, pp. 2690–2699, July 2007.

[25] N. C. Beaulieu, A. Abu-Dayya, and P. McLance, "Estimating the distribution of a sum of independent lognormal random variables," *IEEE Trans. Commun.*, vol. 43, pp. 2869–2873, Dec. 1995.

[26] "Evolved universal terrestrial radio access (E-UTRA); physical layer procedures (release 8)," Tech. Rep. 36.213 (v8.3.0), 3rd Generation Partnership Project (3GPP), 2008.
[27] D. Tse and P. Vishwanath, *Fundamentals of Wireless Communications*. Cambridge University Press, 2005.
[28] J. G. Choi and S. Bahk, "Cell-throughput analysis of the proportional fair scheduler in the single-cell environment," *IEEE Trans. Veh. Technol.*, vol. 56, pp. 766–778, Mar. 2007.
[29] A. Jalali, R. Padovani, and R. Pankaj, "Data throughput of CDMA-HDR a high efficiency-high data rate personal communication wireless system," in *Proc. VTC (Spring)*, pp. 1854–1858, May 2000.
[30] E. Liu and K. K. Leung, "Expected throughput of the proportional fair scheduling over Rayleigh fading channels," *IEEE Commun. Lett.*, vol. 14, pp. 515–517, June 2010.
[31] J. Wu, N. B. Mehta, A. F. Molisch, and J. Zhang, "Unified spectral efficiency analysis of cellular systems with channel-aware schedulers," to appear in *IEEE Trans. Commun.*, 2011.
[32] G. Fishman, *Monte Carlo: Concepts, Algorithms, and Applications*, 1st edition. Springer, 1996.
[33] T. D. Pham and K. G. Balmain, "Multipath performance of adaptive antennas with multiple interferers and correlated fadings," *IEEE Trans. Veh. Technol.*, vol. 48, pp. 342–352, Mar. 1999.
[34] J. H. Winters, "Optimum combining in digital mobile radio with cochannel interference," *IEEE Trans. Veh. Technol.*, vol. 33, pp. 144–155, Aug. 1984.
[35] M. Simon and M.-S. Alouini, *Digital Communication over Fading Channels*, 2nd edition. Wiley-Interscience, 2005.
[36] T. M. Cover and J. A. Thomas, *Elements of Information Theory*. Wiley Series in Telecommunications, 1991.
[37] M. Assaad and A. Mourad, "New frequency-time scheduling algorithms for 3GPP/LTE-like OFDMA air interface in the downlink," in *Proc. VTC (Spring)*, pp. 1964–1969, May 2008.
[38] NTT DoCoMo, Fujitsu, Mitsubishi Electric Corporation, NEC, QUALCOMM Europe, Sharp, Toshiba Corporation, "Adaptive modulation and channel coding rate control for single-antenna transmission in frequency domain scheduling," R1-060039, 3GPP RAN1 LTE Ad Hoc Meeting, Jan. 2006.
[39] NTT DoCoMo, "Investigations on codebook size for MIMO precoding in E-UTRA downlink," R1-070093, 3GPP RAN1 #47, Jan. 2007.
[40] T. Tang, C. Chae, R. Heath, S. Cho, and S. Yun, "Opportunistic scheduling in multiuser OFDM systems with clustered feedback," *Wireless Pers. Commun.*, vol. 52, pp. 209–225, June 2008.
[41] M.-S. Alouini and A. Goldsmith, "Area spectral efficiency of cellular mobile radio systems," *IEEE Trans. Veh. Technol.*, vol. 48, pp. 1047–1066, 1999.
[42] A. M. Tulino and S. Verdu, *Random Matrix Theory and Wireless Communications*. Now Publishers Inc., 2004.
[43] M. Abramowitz and I. Stegun, *Handbook of Mathematical Functions with Formulas, Graphs, and Mathematical Tables*, 9th edition. Dover, 1972.
[44] K. L. Baum, T. A. Kostas, P. J. Sartori, and B. K. Classon, "Performance characteristics of cellular systems with different link adaptation strategies," *IEEE Trans. Veh. Technol.*, vol. 52, pp. 1497–1507, Nov. 2003.

Sushruth N. Donthi received his Bachelor of Engineering degree in Telecommunications Engineering from Vemana Institute of Technology, Bangalore in 2006. He received his Master of Science degree from the Dept. of Electrical Communication Engineering, Indian Institute of Science, Bangalore, India in 2011. Since then, he has been with Broadcom Communications Technologies Pvt. Ltd., Bangalore, India working on design and implementation of parts of the LTE protocol stack. From 2006-2008, he was at LG Soft India Pvt. Ltd., working on software development for 3G handsets. His research interests include the design and analysis of algorithms for wireless cellular systems, communication networks and MIMO systems.

Neelesh B. Mehta (S'98-M'01-SM'06) received his Bachelor of Technology degree in Electronics and Communications Engineering from the Indian Institute of Technology (IIT), Madras in 1996, and his M.S. and Ph.D. degrees in Electrical Engineering from the California Institute of Technology, Pasadena, CA, USA in 1997 and 2001, respectively. He is now an Assistant Professor in the Dept. of Electrical Communication Eng., Indian Institute of Science (IISc), Bangalore, India. Prior to joining IISc, he was a research scientist in the Wireless Systems Research group in AT&T Laboratories, Middletown, NJ, USA from 2001 to 2002, Broadcom Corp., Matawan, NJ, USA from 2002 to 2003, and Mitsubishi Electric Research Laboratories (MERL), Cambridge, MA, USA from 2003 to 2007.

His research includes work on link adaptation, multiple access protocols, WCDMA downlinks, system-level performance analysis of cellular systems, MIMO and antenna selection, and cooperative communications. He was also actively involved in the Radio Access Network (RAN1) standardization activities in 3GPP from 2003 to 2007. He has served on several TPCs. He was a TPC co-chair for WISARD 2010 and 2011, National Conference on Communications (NCC) 2011, the Transmission Technologies track of VTC 2009 (Fall), and the Frontiers of Networking and Communications symposium of Chinacom 2008. He was the tutorials co-chair for SPCOM 2010. He has co-authored 25 IEEE journal papers, 55 conference papers, and two book chapters, and is a co-inventor in 16 issued US patents. He is an Editor of the IEEE TRANSACTIONS ON WIRELESS COMMUNICATIONS and is an executive committee member of the IEEE Bangalore Section and the Bangalore chapter of the IEEE Signal Processing Society.